

## Nonlinear Observer-Based Control for Grid Connected Photovoltaic System

M'hammed Guisser<sup>1\*</sup>, Elhassane Abdelmounim<sup>1</sup>, Mohammed Aboufatah<sup>1</sup>,  
Abdesselam EL-Jouni<sup>2</sup>

<sup>1\*</sup>(Department of Electrical Engineering, CRMEF-Settat.ASTI Laboratory, FST Settat, University Hassan I, Morocco)

<sup>1</sup>(ASTI Laboratory, FST Settat, University Hassan I, Morocco)

<sup>2</sup>(Department of Physics Faculty of Science Dhar El-Mehraz Fes, Morocco)

---

**Abstract:** A new nonlinear observer-based control scheme for a single-phase photovoltaic (PV) system connected to the grid is presented. The system consists of a PV array, DC-DC Boost converter and a DC-AC inverter coupled to grid network. The DC-DC converter is used to extract maximum power from the PV array and the DC-AC inverter is used to synchronize a sinusoidal current output with a voltage grid with regulated DC bus voltage. A robust nonlinear controller is developed using the sliding mode control design technique based on an averaged nonlinear model of the whole controlled system. The control action is carried out assuming that all the states of the grid connected PV system are known by measurement. Then, a nonlinear state observer for Boost inductor current, DC bus voltage and grid injected current estimation is implemented from the measurement of PV array voltage state, PV array current signal and grid voltage signal. The observer-based control method provides robust maximum power point tracking (MPPT), grid current tracking and DC bus voltage regulation, achieves unity power factor and optimizes the PV energy extraction suitable for grid connected PV systems. Simulation results are provided to demonstrate the effectiveness of the proposed design and robustness under different operating conditions such as changes in atmospheric conditions and noise measurements.

**Keywords:** Grid connected photovoltaic system, Maximum power point tracking (MPPT), DC-DC converter, DC-AC inverter, Sliding mode control, asymptotic stability, State observer

---

### I. Introduction

The much concerned with the fossil fuel exhaustion and the environmental problems are caused by the conventional power generation. Nowadays, renewable energy sources, such as photovoltaic (PV) panels, biomass and wind-generators, are now widely used. Among these, solar energy is considered to be one of the most useful sources because it is free, abundant, pollution free and maintenance free. PV sources are used today in many applications such as domestic equipments, computers, industrial electronics, battery operating portable equipments, water pumping and uninterruptible power sources. Since the generated voltage from PV is DC, we need inverter for converting DC voltage from PV to AC before connecting it to grid. The output voltage and frequency of inverter should be same as that of grid frequency and voltage.

Among the PV energy applications, they can be divided into two categories: one is standalone system and the other is grid-connected system. Stand-alone system requires the battery bank to store the PV energy which is suitable for low-power system. On the other hands, grid-connected system does not require the battery bank and has become the primary PV application for high power applications. The main purpose of the grid-connected system is to transfer maximum solar array energy into grid with a unity power factor.

Grid-connected PV system has gained popularity due to the feed-in-tariff and the reduction of battery cost. However, the operating point of PV generator varies with the load and the change in atmospheric conditions. Maximum power point tracking (MPPT) techniques are used to deliver maximum power into the grid. Efficient and advanced control schemes are essential to ensure maximum power output of a PV system at different operating conditions. Several MPPT algorithms have been proposed, Perturb and Observe (P&O) [1], Incremental Conductance [2], fuzzy based algorithms [3]. They differ from its complexity and tracking accuracy but they all required sensing the PV current and/or the PV voltage.

An interesting solution to ensure the operation of grid connected photovoltaic systems over a wide range of operating points, the design and implementation of nonlinear controller approaches, such as sliding mode control [4], [5], [6], backstepping control [7], [8], [9].

Single-phase grid connected PV systems have advantages such as simple topology, high efficiency. The inverter is the key-component for successful operation of the grid connected PV system. It utilize various control strategy; power controlled [10], current controlled grid connected PV system [11].

However, most of the above works need continuous measurements of AC voltages, AC currents and DC voltage, DC current. This requires a large number of both voltage and current sensors, which increases system complexity, cost, space, and reduces system reliability. Moreover, the sensors are susceptible to electrical noise, which cannot be avoided during high-power switching. Reducing the number of sensors has a significant affect upon the control system's performance. The use of sensors in the control architecture inherently increases the possibility of failure and increases the cost (measurement noise, sensor calibration and accuracy, data acquisition and processing, etc.) of the control system due to the additional hardware. Hence, the use of an observer in the control loop to complete the measurement of the state variables. A few results have been proposed to reduce the current sensors [12].

In this paper, a new observer-based control without boost converter current, DC bus voltage and grid current measurement has been proposed. These informations are obtained from the state observer and injected into the control law, the state observer has been constructed from the system dynamic equation of grid connected PV system. For control schemes, two control signals are employed for grid connected PV system. The first control signal regulates the DC-DC converter to extract maximum output power from the PV array. The second control signal regulates the DC-AC inverter to generate grid current controlled sinusoidal with unity power factor and ensuring a tight regulation of the DC-bus voltage and transforming the maximum output power into the grid. The control is designed using robust sliding mode control to permit a direct control of power converters.

The rest of the paper is organized as follows. The state space dynamic model of the global grid connected PV system is described in Section II. The controller design for grid connected photovoltaic system is presented in Section VI. In Section III, a high gain state observer is developed to estimate the unmeasured states. Simulation results and their comments are illustrated in Section V. Finally, the paper is concluded in Section VI.

## II. Mathematical Modeling of the Grid Connected PV System

Grid connected PV generator systems always a connection to the electrical network via a suitable inverter because a PV module delivers only DC power. Fig. 1 shows the configuration of the single-phase grid connected PV generation system. PV array is connected to the DC bus via a DC-DC boost converter, and then to the AC grid via a DC-AC inverter. The boost converter is used for boosting the array voltage and achieving maximum power point tracking for the PV array. The inverter with filter inductor converts a DC input voltage into an AC sinusoidal by means of appropriate switch signals to make the output current in phase with the utility voltage and so obtain a power factor unity.

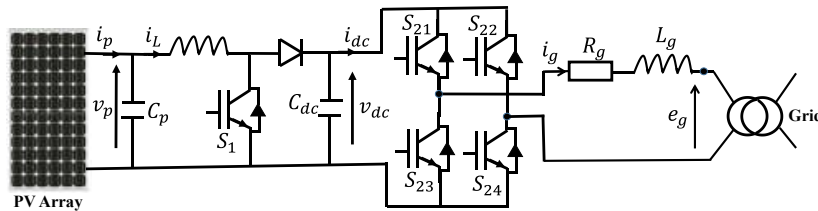


Fig.1. Single-phase grid connected PV system.

### 2.1. PV Array Modelling

PV cell is a simple p-n junction diode which converts the irradiation into electricity. Fig. 2 shows an equivalent circuit diagram of a PV cell which consists of a light generated current source  $I_{ph}$ , a parallel diode, shunt resistance  $R_{sh}$  and series resistance  $R_s$ .

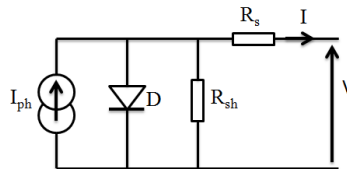


Fig.2. Equivalent circuit diagram of PV cell.

The characteristic equation of the PV cell current  $i_p$  and PV voltage cell  $v_p$  is given as follows:

$$i_p = I_{ph} - I_s \left[ \exp \left( \frac{v_p + R_s i_p}{\gamma V_T} \right) - 1 \right] - \frac{v_p + R_s i_p}{R_{sh}} \quad (1)$$

where  $I_s$  is the saturation current,  $V_T = K_B T/q$  is the thermal voltage,  $K_B$  is the Boltzmann's constant,  $q$  is the charge of electron,  $T$  is the cell's absolute working temperature,  $\gamma$  is the p-n junction ideality factor.

The light generated current  $I_{ph}$  depends on the solar irradiation and temperature, which can be related by the following equation:

$$I_{ph} = [I_{scr} + K_i(T - T_r)] \frac{G}{1000} \quad (2)$$

where,  $I_{scr}$  is the short circuit current,  $G$  is the solar irradiation,  $K_i$  is the cell's short circuit current coefficient and  $T_r = 298.15K$  is the reference temperature of the cell.

The cell's saturation current  $I_s$  varies with the temperature according to the following equation:

$$I_s = I_{rr} \left[ \frac{T}{T_r} \right]^3 \left[ \exp \frac{qE_G}{\gamma K_B} \left( \frac{1}{T_r} - \frac{1}{T} \right) \right] \quad (3)$$

where,  $E_G$  is the band-gap energy of the semiconductor used in the cell and  $I_{rr}$  is the reverse saturation current of the cell at reference temperature and solar irradiation.

Since the output voltage of PV cell is very low, a number of PV cells are connected together in series in order to obtain higher voltages. A number of PV cells are put together and encapsulated with glass, plastic, and other transparent materials to protect from harsh environment, to form a PV module. To obtain the required voltage and power, a number of modules are connected in parallel to form a PV array. The mathematical equation relating the PV array current to the PV array voltage becomes:

$$i_p = N_p I_{ph} - N_p I_s \left[ \exp \frac{1}{\gamma V_T} \left( \frac{v_p}{N_s} + \frac{R_s i_p}{N_p} \right) - 1 \right] - \frac{N_p}{R_{sh}} \left( \frac{v_p}{N_s} + \frac{R_s i_p}{N_p} \right) \quad (4)$$

where  $N_s$  is the number of cells in series and  $N_p$  is the number of modules in parallel.

The PV array module considered in this paper is the Siemens SM55. The corresponding electrical characteristics are listed in Table 1. The associated current-voltage and power-voltage characteristics under changing climatic conditions (temperature and radiation) are shown in Figs. 3 and 4.

Nominal voltage	12V
Maximum power	55W
Current at the maximum power point	3.15A
Voltage at the maximum power point	17.4V
Maximum current (short circuit output)	3.45A
Maximum voltage (open circuit)	21.7V
Current temperature coefficient	+1.2mA/°C
Number of series cells $N_s$	36
Number of parallel modules $N_p$	1

**Table1:** Parameter of the PV array SIEMENS SM55.

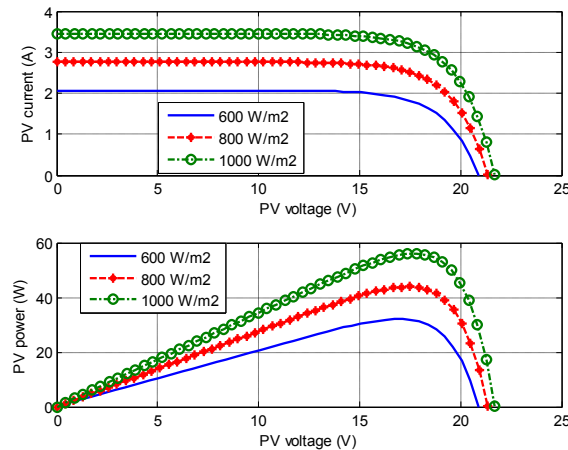


**Fig.3.** PV array current–voltage and PV array power–voltage at 25°C at different irradiance levels.

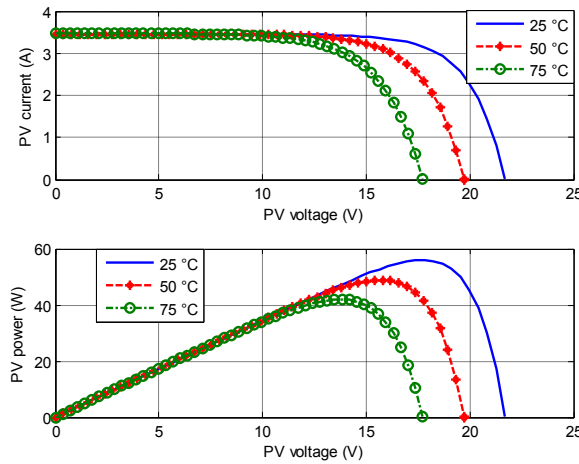


Fig.4. PV array current–voltage and PV array power–voltage at 1000W/m<sup>2</sup> at different temperature levels.

Based on the solar array characteristic curves shown in Figs. 3 and 4 when the solar array is operating in its maximum output power  $P = v_p i_p$ , we can get:

$$\frac{\partial P}{\partial v_p} = \frac{\partial (v_p i_p)}{\partial v_p} = i_p + v_p \frac{\partial i_p}{\partial v_p} = 0 \quad (5)$$

### 2.2. Grid Connected PV System Modelling

For a control scheme to be effective for single-phase grid connected PV system, some details of the system is essential. The details of any system can best be described by the mathematical model. The control inputs  $\mu_1$  and  $\mu_2$  respectively of the boost converter and the inverter are pulse width modulation (PWM). The binary input switching signals can be defined as follows:

$$\begin{cases} \mu_1 = 1 \text{ if } S_1: \text{ on} \\ \mu_1 = 0 \text{ if } S_1: \text{ off} \end{cases} \quad (6)$$

$$\begin{cases} \mu_2 = 1 \text{ if } S_{21}, S_{24}: \text{ on. } S_{22}, S_{23}: \text{ off} \\ \mu_2 = 0 \text{ if } S_{21}, S_{24}: \text{ off. } S_{22}, S_{23}: \text{ on} \end{cases} \quad (7)$$

The state space dynamic model of grid connected PV system can be obtained using the state averaging equation described as follows:

$$\begin{cases} \frac{dv_p}{dt} = \frac{1}{C_p} i_p - \frac{1}{C_p} i_L \\ \frac{di_L}{dt} = \frac{1}{L} v_p - \frac{1}{L} (1 - u_1) v_{dc} \\ \frac{dv_{dc}}{dt} = \frac{1}{C_{dc}} (1 - u_1) i_L + \frac{1}{C_{dc}} (1 - 2u_2) i_g \\ \frac{di_g}{dt} = -\frac{1}{L_g} R_g i_g - \frac{1}{L_g} e_g - \frac{1}{L_g} (1 - 2u_2) v_{dc} \\ y_1 = \frac{\partial P}{\partial v_p} = i_p + v_p \frac{\partial i_p}{\partial v_p} \\ y_2 = i_g \end{cases} \quad (8)$$

where  $C_p$  is the input capacitor and  $L$  is the inductor of the boost converter.  $C_{dc}$  is the DC link capacitor,  $L_g$  is the filter inductor and  $R_g$  is the equivalent series resistance of the filter inductor.  $i_p$ ,  $v_p$ ,  $i_L$ ,  $v_{dc}$ ,  $i_g$  and  $e_g$  are respectively, the average values over switching period of the PV array current, PV array voltage, boost inductor current, DC bus voltage, grid current and grid voltage. The control inputs  $u_1$  and  $u_2$  are the average values (duty cycles) of the binary input switching signals  $\mu_1$  and  $\mu_2$ .

The mathematical model of single-phase grid connected PV system can be expressed as the following form of multi-input multi-output (MIMO) nonlinear system:

$$\begin{cases} \dot{x} = f(x) + g_1(x)u_1 + g_2(x)u_2 \\ y = h(x) \end{cases} \quad (9)$$

where  $x = [v_p \ i_L \ v_{dc} \ i_g]^T$  is the state vector,  $u = [u_1 \ u_2]^T$  is the control input vector and  $y = [y_1 \ y_2]^T = [h_1(x) \ h_2(x)]^T = \left[ \frac{\partial P}{\partial v_p} \ i_g \right]^T$  is the output vector to be controlled. The vector function  $f(x)$  and the matrix  $g(x) = [g_1(x) \ g_2(x)]$  are defined as follows:

$$f(x) = \begin{pmatrix} \frac{1}{C_p} i_p - \frac{1}{C_p} i_L \\ \frac{1}{L} v_p - \frac{1}{L} v_{dc} \\ \frac{1}{C_{dc}} i_L + \frac{1}{C_{cd}} i_g \\ -\frac{1}{L_g} R_g i_g - \frac{1}{L_g} e_g - \frac{1}{L_g} v_{dc} \end{pmatrix}, g_1(x) = \begin{pmatrix} 0 \\ \frac{1}{L} v_{dc} \\ -\frac{1}{C_{cd}} i_L \\ 0 \end{pmatrix} \text{ and } g_2(x) = \begin{pmatrix} 0 \\ 0 \\ -\frac{2}{C_{cd}} i_g \\ \frac{2}{L_g} v_{dc} \end{pmatrix}$$

### III. Nonlinear Control Design

Two main objectives have to be fulfilled in order to transfer efficiently the photovoltaic generated energy into the utility grid are tracking the PV's maximum power point (MPP) and obtain unity power factor and low harmonic distortion at the output. To accomplish the previous objectives. Switch  $S_1$  of the boost converter is governed by control signal  $u_1$  generated by the controller that deals exclusively with the photovoltaic array's maximum power point tracking (MPPT). The unity power factor controller signal  $u_2$  that controls switch arms ( $S_{21}, S_{24}$ ) and ( $S_{22}, S_{23}$ ) of the inverter. A sliding mode controller technique has been chosen given that it has shown good performances and robustness under the presence of parameter variations and disturbance. The control law is carried out assuming that all the state variables are known by measurement.

#### 3.1. MPPT Controller Of The Boost Converter

The boost converter is governed by control signal  $u_1$  generated by the sliding mode controller that allow to extract maximum power of photovoltaic generator control by regulating the controlled output  $y_1 = h_1(x) = \frac{\partial P}{\partial v_p}$  of the photovoltaic array to its reference  $y_{1ref} = \frac{\partial P}{\partial v_p} \Big|_{MPP} = 0$ .

Consider grid connected PV System equations (8) and (9). Differentiating the controlled output  $y_1 = h_1(x)$  with respect to time yields:

$$\dot{y}_1 = \frac{\partial h_1}{\partial x} \dot{x} = \frac{\partial h_1}{\partial x} (f(x) + g(x)u) = L_f h_1(x) + L_{g_1} h_1(x)u_1 + L_{g_2} h_1(x)u_2 \quad (10)$$

where:

$$L_f h_1(x) = \left( 2 \frac{\partial i_p}{\partial v_p} + v_p \frac{\partial^2 i_p}{\partial v_p^2} \right) \frac{dv_p}{dt} \text{ and } L_{g_1} h_1(x) = L_{g_2} h_1(x) = 0.$$

The functions  $L_f h_1(x)$  and  $L_{g_1} h_1(x)$  are called the Lie Derivative of  $h_1(x)$  along  $f(x)$  and  $g(x)$  respectively.

Continuing the differentiation of the output  $y_1 = h_1(x)$  with respect to time :

$$\ddot{y} = L_f^2 h_1(x) + L_{g_1} L_f h_1(x)u_1 \quad (11)$$

where:

$$L_f^2 h_1(x) = \left( 3 \frac{\partial^2 i_p}{\partial v_p^2} + v_p \frac{\partial^3 i_p}{\partial v_p^3} \right) \left( \frac{dv_p}{dt} \right)^2 + \left( 2 \frac{\partial i_p}{\partial v_p} + v_p \frac{\partial^2 i_p}{\partial v_p^2} \right) \left[ \frac{1}{C_p} \frac{\partial i_p}{\partial v_p} \frac{dv_p}{dt} - \frac{1}{LC_p} (v_p - v_{dc}) \right]$$

and

$$L_{g_1} L_f h_1(x) = -\frac{1}{LC_p} \left( 2 \frac{\partial i_p}{\partial v_p} + v_p \frac{\partial^2 i_p}{\partial v_p^2} \right) v_{dc}$$

The relative degree of the output function  $y_1 = h_1(x)$ , is  $r_1 = 2$ . The sliding surface can be designed with the tracking error between the controlled output and its reference  $e_1 = y_1 - y_{1ref}$ . The switching surface is defined by:

$$\sigma_1 = \dot{e}_1 + \lambda_1 e_1 \quad (12)$$

where  $\lambda_1 > 0$ .

Differentiation of the sliding surface yields:

$$\dot{\sigma}_1 = \ddot{e}_1 + \lambda_1 \dot{e}_1 \quad (13)$$

Substituting equation (11) in equation (13), we have:

$$\dot{\sigma}_1 = L_f^2 h_1(x) + L_{g_1} L_f h_1(x)u_1 + \lambda_1 L_f h_1(x) \quad (14)$$

For equation (13), a candidate Lyapunov function is introduced taking the form:

$$V_1 = \frac{1}{2} \sigma_1^2 \quad (15)$$

In order to provide the asymptotic stability of equation (13) about the equilibrium point  $\sigma_1 = 0$ , the following conditions must be satisfied  $\dot{V}_1 < 0$ . Selecting the time derivative of the switching surface as:

$$\dot{\sigma}_1 = -\Gamma_1 \text{sign}(\sigma_1) \quad (16)$$

where  $\Gamma_1$  is a strictly positive constant and sign is the signum function which ensures that:

$$\dot{V}_1 = -\Gamma_1 |\sigma_1| < 0 \quad (17)$$

Therefore, the control input  $u_1$  that is computed to satisfy equation (16) will drive the controlled output  $y_1$  to zero in finite time and will keep it at zero thereafter is given by:

$$u_1 = \frac{1}{L_{g1}L_f h_1(x)} [-L_f^2 h_1(x) - \lambda_1 L_f h_1(x) - \Gamma_1 \text{sign}(\sigma_1)] \quad (18)$$

### 3.2. Unity Power Factor Controller of the Inverter

This controller synthesis consists of an inner current loop and an outer voltage loop [8], [9]. The inner current loop is designed using sliding mode control to obtain a unitary power factor and to inject a sinusoidal current in the network. The outer voltage loop is designed by a simple proportional-integral (PI) corrector to generate the reference grid current signal  $i_{gref}$ , which will be used by the inner current loop controller and to regulate the DC bus voltage at its desired reference value  $v_{dcref}$ .

The inner current loop controls the output current  $i_g$  to the shape and phase of the utility grid voltage  $e_g$  by generating a control signal  $u_2$ . Thus, the output current  $i_g$  needs to track a scaled utility grid voltage, that is, the following current reference signal:

$$i_{gref} = \beta e_g \quad (19)$$

where  $\beta$  is a time-varying real positive parameter generated by the PI controller.

Assuming that the utility grid voltage has a sinusoidal shape, equation (19) can be rewritten as follows:

$$i_{gref} = \beta E\sqrt{2}\sin(\omega t) \quad (20)$$

where  $E\sqrt{2}$  represents the utility grid's amplitude and  $\omega = 2\pi f$  is the angular frequency of the grid,  $f$  is the grid frequency.

Differentiating the controlled output  $y_2 = h_2(x) = i_g$  with respect to time:

$$\dot{y}_2 = L_f h_2(x) + L_{g1} h_2(x)u_1 + L_{g2} h_2(x)u_2 \quad (21)$$

where:

$$L_f h_2(x) = \frac{1}{L_g} (-R_g i_g - e_g - v_{dc}), L_{g1} h_2(x) = 0 \text{ and } L_{g2} h_2(x) = \frac{2}{L_g} v_{dc}.$$

The relative degree of the output function  $y_2 = h_2(x)$ , is  $r_2 = 1$ . The following sliding surface is proposed for the inner control loop:

$$\sigma_2 = i_g - i_{gref} \quad (22)$$

The sliding surface in (22) assures that when the sliding motion is reached the grid current  $i_g$  will track the reference signal  $i_{gref}$  defined in (20). According to the dynamic of the sliding surface:

$$\dot{\sigma}_2 = -\Gamma_2 \text{sign}(\sigma_2) \quad (23)$$

where  $\Gamma_2$  is a positive parameter. The derivative of the Lyapunov function  $V_2 = \frac{1}{2}\sigma_2^2$  is computed as  $\dot{V}_2 = -\Gamma_2|\sigma_2| < 0$ . Consequently the control law  $u_2$  that drives the grid current  $i_g$  to the reference signal in finite time is:

$$u_2 = \frac{1}{L_{g2} h_2(x)} \left[ -L_f h_2(x) + \frac{di_{gref}}{dt} - \Gamma_2 \text{sign}(\sigma_2) \right] \quad (24)$$

The aim of the outer voltage loop is to generate a tuning law for the ratio  $\beta$  in such a way that the DC bus voltage  $v_{dc}$  be regulated to a given reference value  $v_{dcref}$ . The DC bus voltage is set by a PI controller that compares the actual DC bus voltage and its reference to generate the reference grid current. The outer voltage loop controller is defined by:

$$\beta(t) = k_1 \varepsilon_{dc}(t) + k_2 \int_0^t \varepsilon_{dc}(\tau) d\tau \quad (25)$$

where  $\varepsilon_{dc} = v_{dc} - v_{dcref}$ ,  $k_1$  is the proportional gain and  $k_2$  is the integral gain.

The block diagram of the outer loop controller is shown in Fig. 5.

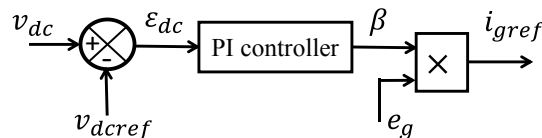


Fig. 5. Blok diagram for regulating the DC bus voltage

### IV. Nonlinear State Observer Design

In practice it is rarely the full state variables of the system are available for feedback. A possible solution to this problem is the use of an observer. An observer can generate an estimate of the full state using knowledge of the available measurements output and input of the system. The proposed nonlinear observer is employed to estimate boost inductor current, DC bus voltage and grid current only from the measurement of PV array voltage state, PV array current signal and grid voltage signal.

The grid connected PV system (9) can be represented in a general form which belong to the class of state affine systems uniformly observable allowing the synthesis of the state observer [13], [14], [15], [16], [17].

$$\begin{cases} \dot{x}_1 = a_1(u)x_2 + \varphi_1(x_1, u, s) \\ \dot{x}_2 = a_2(u)x_3 + \varphi_2(x_1, x_2, u, s) \\ \dot{x}_3 = a_3(u)x_4 + \varphi_3(x_1, x_2, x_3, u, s) \\ \dot{x}_4 = \varphi_4(x_1, x_2, x_3, x_4, u, s) \\ y_m = x_1 \end{cases} \quad (26)$$

with:

$$a_1(u) = -\frac{1}{C_p}, \quad a_2(u) = -\frac{1}{L}(1 - u_1); \quad a_3(u) = \frac{1}{C_{cdc}}(1 - 2u_2); \quad \varphi_1(x, u, s) = \frac{1}{C_p}i_p; \quad \varphi_2(x, u, s) = \frac{1}{L}x_1; \\ \varphi_3(x, u, s) = \frac{1}{C_{dc}}(1 - u_1)x_2; \quad \varphi_4(x, u, s) = \frac{1}{L_g}[-R_g x_4 - e_g - (1 - 2u_2)x_3].$$

where  $x$  is the state variables vector,  $u$  is the control input vector,  $y_m$  is the measured output that represents the PV array voltage state and  $s = (i_p, e_g)$  is a knowing signal.

The grid connected PV system (26) can be represented in a more general observable canonical form given by:

$$\begin{cases} \dot{x} = A(u) + \varphi(x, u, s) \\ y_m = Cx \end{cases} \quad (27)$$

where:

$$A(u) = \begin{bmatrix} 0 & a_1(u) & 0 & 0 \\ 0 & 0 & a_2(u) & 0 \\ 0 & 0 & 0 & a_3(u) \\ 0 & 0 & 0 & 0 \end{bmatrix}, \quad C = [1 \ 0 \ 0 \ 0] \text{ and } \varphi(x, u, s) = [\varphi_1 \ \varphi_2 \ \varphi_3 \ \varphi_4]^T.$$

Assuming that the function  $\varphi(x, u, s)$  is global Lipschitz with respect to  $x$  uniformly in  $u$  and  $s$  [17]. The control input  $u$  is assumed to be regularly persistent [18]. The following dynamical system:

$$\begin{cases} \dot{\hat{x}} = A(u) + \varphi(\hat{x}, u, s) - S^{-1}C^T(C\hat{x} - y_m) \\ \dot{S} = -\theta S - A^T(u)S - SA(u) + C^T C \\ \hat{y}_m = C\hat{x} \end{cases} \quad (28)$$

is an exponential observer for grid connected PV system (27). Furthermore, the estimation error  $\hat{x} - x$  converges exponentially to zero, for  $\theta > 0$  sufficiently large.

where  $\hat{x}$  is the estimation of the full state vector,  $y_m$  is the measured output,  $u$  is the control input of the grid connected PV system,  $S$  is a symmetric positive definite matrix and a solution of the differential Lyapunov equation.

## V. Simulation Results and Discussion

In order to investigate the effectiveness of the proposed observer-based control algorithm of the single-phase grid connected PV system, a group of simulations results has been presented using MATLAB/Simulink environment. The observed states of power system are directly used as the input to the controller where the control law is based on the signals of observer using the measured output of system, and does not need to be expressed in terms of all measured variables as shown in Fig. 6. The parameters of grid connected PV system and the tuning parameters of the controller and observer are summarized in Table 2. The simulation has been performed when solar irradiation changes from 500W/m<sup>2</sup> to 1000W/m<sup>2</sup> at 0.5s and temperature changes from 25°C to 50°C at 1.5s, as shown in Fig. 7. The reference of the DC bus voltage is an echelon going from 40V to 44V at 1s.

The proposed observer-based controller is evaluated from two aspects: robustness to different operating environment conditions (irradiance and temperature) and measurement noise. Two scenarios were simulated. The first (Figs. 8 to 13) corresponds to the estimation of state variables from noise free data of the measured signals. The second (Figs. 14 to 19) corresponds to the estimation of state variables from noisy data of the output measurements: the measured signals are corrupted by an additive Gaussian noise with zero mean and amplitude equivalent to 10% on the corresponding measures.

Fig. 8 shows the PV array power and the first controlled output  $y_1 = \partial P / \partial v_p$  that represents the derivative of PV array power with respect to its voltage. Notice that the maximum power point is always reached very quickly with excellent accuracy after a smooth transient response with good performances. The commanded output reaches the reference value  $y_{1ref} = 0$  according to atmospheric condition changes.

Fig. 9 shows the grid current and the grid voltage, it can be seen that the grid current is sinusoidal and in phase with the grid voltage, this shows that the unity power factor is perfectly realized. Fig. 10 indicates that the injected current to grid tracks the reference value.

Fig. 11 illustrates respectively, the PV array voltage, the PV array current, the boost inductor current and the DC bus voltage. It is noted that the DC bus voltage follows its reference value. From figures 10 and 11, it is clear that the estimated states converge to the actual states and match the desired states. It is also noted from Fig. 12 that the state observer guarantees fast convergence of the estimation error dynamics to zero.

Fig. 13 presents the control inputs and sliding surfaces, when the system is operated at maximum power point and at unity power factor; the sliding surfaces converge to zero.

Finally, Figs. 14 to 19 present the dynamic behaviors of the observer-based control design in the presence of noise measurements, it is clear that the designed approach provides better robustness under varying atmospheric conditions and noise measurements.

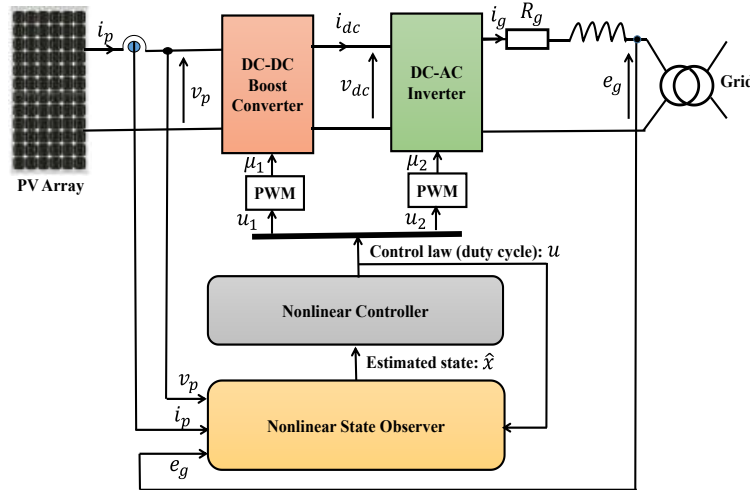


Fig. 6. Schematic diagram of the observer-based control of the grid connected PV system.

Photovoltaic array parameters	Boost converter, inverter and grid parameters	Control and observer parameters
$R_s = 0.1124\Omega$	$C_p = 4700\mu F$	$\lambda = 15$
$R_{sh} = 6500\Omega$	$C_{dc} = 470\mu F$	$\Gamma_1 = 1000$
$\gamma = 1.7404$	$L = 3.5mH$	$\Gamma_2 = 200$
$I_{scr} = 3.45A$	$L_g = 2.2mH$	$k_1 = 0.01$
$I_{rr} = 4.842\mu A$	$R_g = 0.7\Omega$	$k_2 = 1$
$N_s = 36$	$E = 22V$	$\theta = 5$
$N_p = 1$	$f = 50Hz$	

Table 2: Power system and observer-controller parameters.

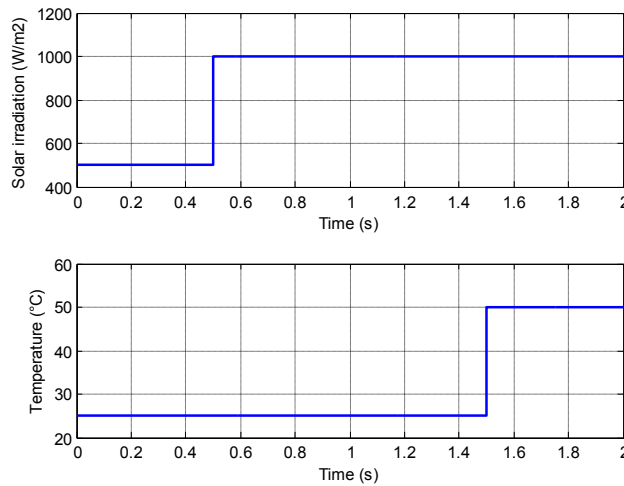


Fig. 7. Change of solar irradiation and temperature.



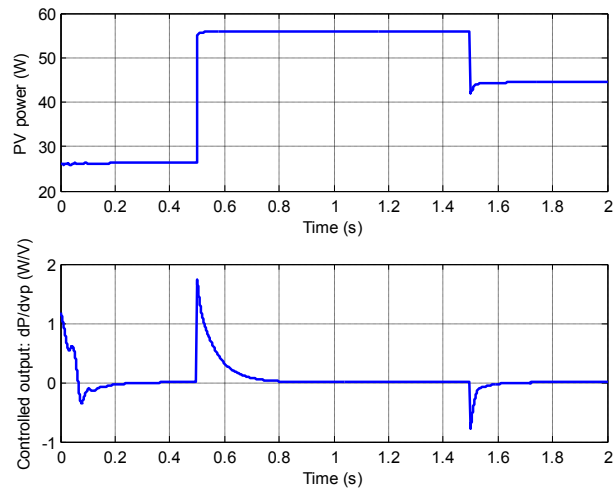


Fig. 8. PV array power and controlled output  $\partial P / \partial v_p$  (without noisy measurements).

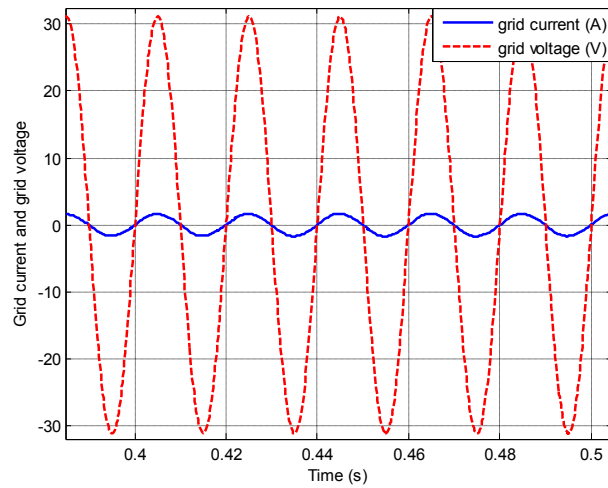


Fig. 9. Grid current and grid voltage (without noisy measurements).

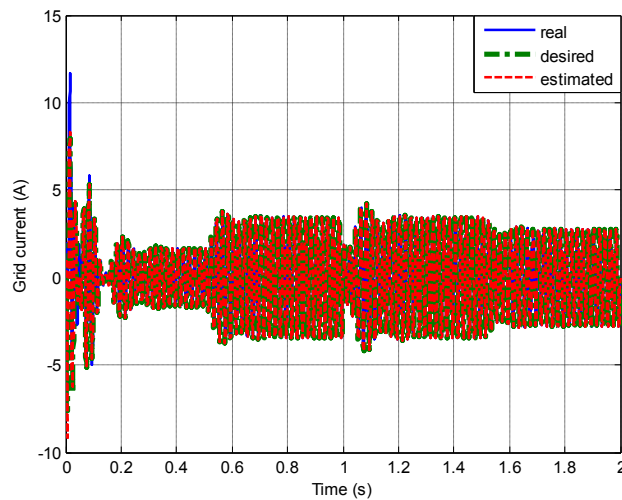


Fig. 10. Grid current (without noisy measurements).

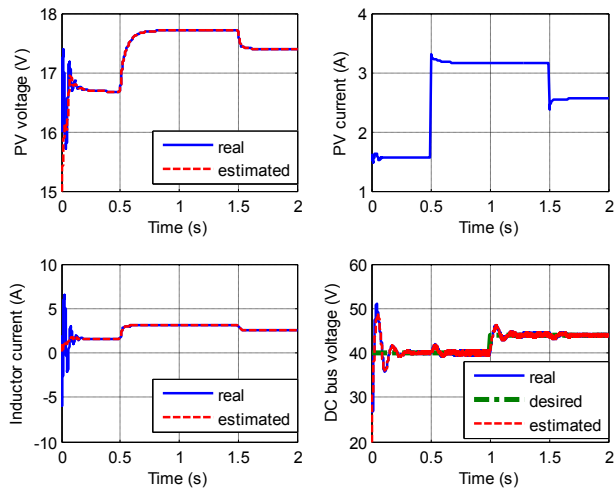


Fig. 11. PV array voltage, PV array current, boost inductor current and DC bus voltage (without noisy measurements).

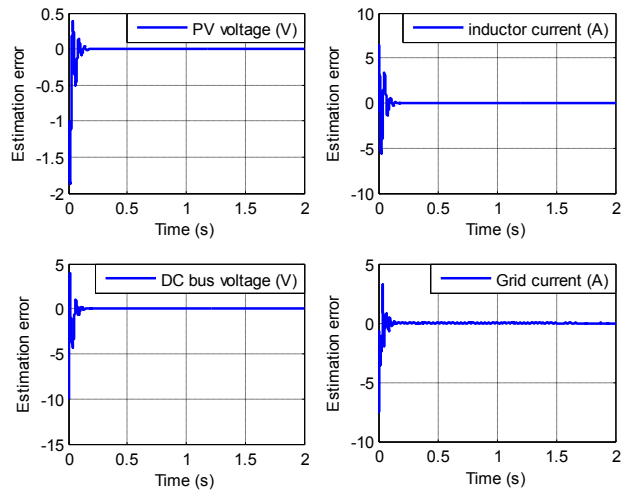


Fig. 12. Estimation error of the state variables (without noisy measurements).

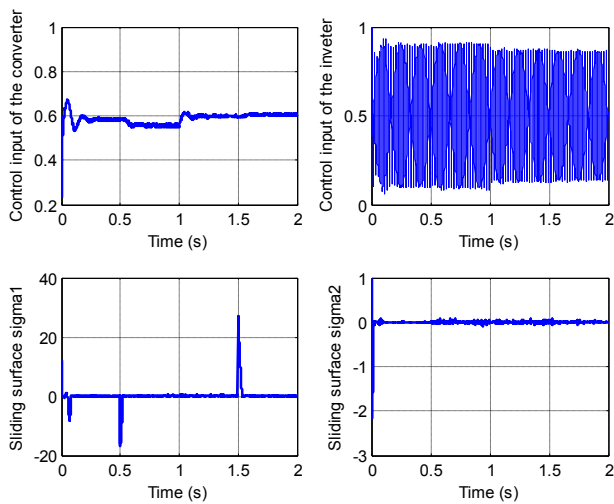


Fig. 13. Control inputs and sliding surfaces (without noisy measurements).

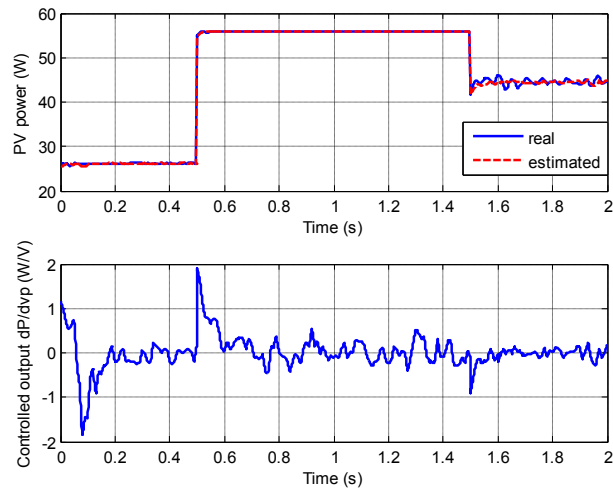


Fig. 14. PV array power and controlled output  $\partial P / \partial v_p$  (with noisy measurements).

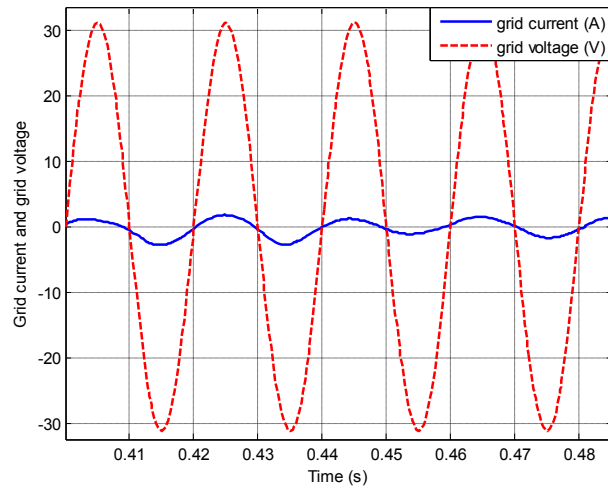


Fig. 15. Grid current and grid voltage (with noisy measurements).

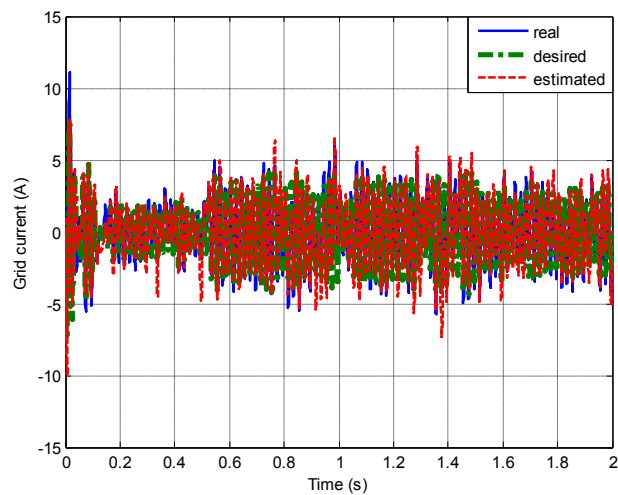


Fig. 16. Grid current (with noisy measurements).

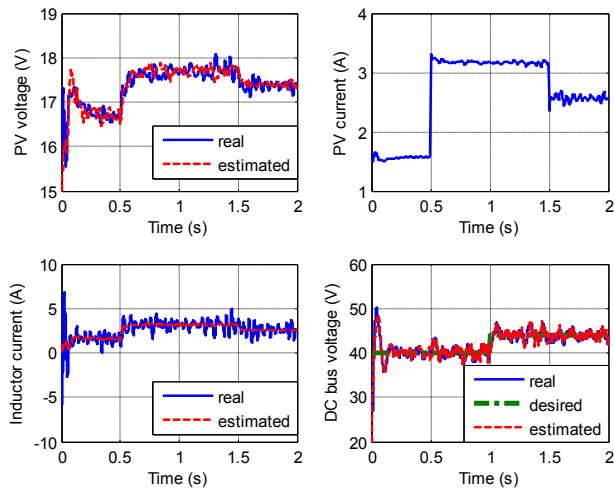


Fig. 17. PV array voltage, PV array current, boost inductor current and DC bus voltage (with noisy measurements).

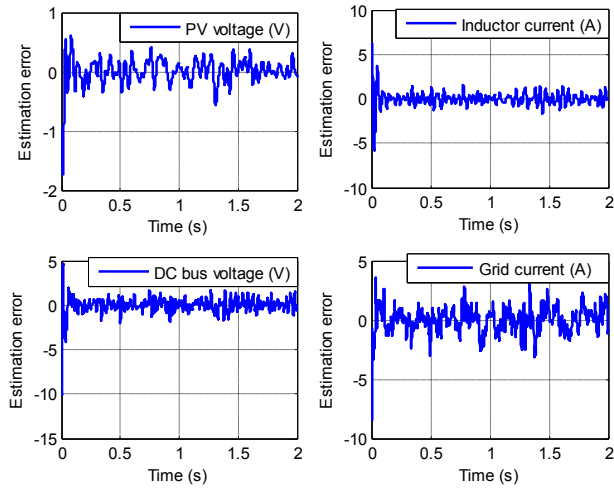


Fig. 18. Estimation error of the state variables (with noisy measurements).

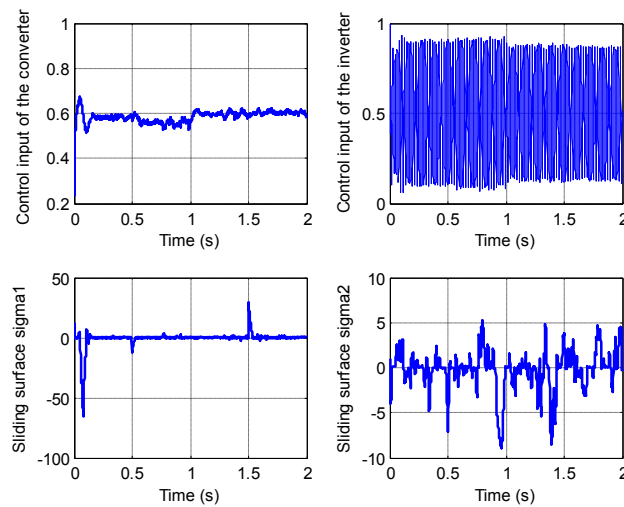


Fig.19. Control inputs and sliding surfaces (with noisy measurements).

## VI. Conclusion

A new nonlinear observer-based control is proposed in this paper for the grid connected PV system. The use of observer reduces the number of current and voltage sensors, decreases the system cost, volume and less sensitive to the noise measurements and facilitates the implementation of the control. A nonlinear sliding mode controller is designed to extract maximum power from the PV array and to inject a sinusoidal current in the grid with unity power factor and regulating the DC bus voltage between the boost converter stage and the inverter stage of the grid connected PV system. Simulation results are provided to verify the effectiveness and robustness of the proposed observer-based control under varying atmospheric conditions and noise measurements.

## References

- [1] N. Femia, G. Petrone, G. Spagnuolo, and M. Vitelli, Optimization of Perturb and Observe maximum power point tracking method, *Power Electronics*, IEEE Transactions, Vol. 20, n.4, July 2005, pp. 963–973.
- [2] Jae Ho Lee; HyunSuBae; Bo Hyung Cho, Advanced Incremental Conductance MPPT Algorithm with a Variable Step Size, *Power Electronics and Motion Control Conference EPEPEMC 12th International*, Sept 2006, pp. 603 – 607.
- [3] NoppornPatcharaprakiti, SuttichaiPremrudeepreechacharn, YosanaoSriuthaisiriwong, Maximum power point tracking using adaptive fuzzy logic control for grid-connected photovoltaic system, *Renewable Energy*, Vol 30 n.11, Sept 2005, pp. 1771–1778.
- [4] HazemFeshara, Mohamed Elharony, SolimanSharaf, Design, Digital Control, and Simulation of a GridConnected Photovoltaic Generation System. *International Journal of Renewable Energy Research*, Vol.4, No.2, 2014.
- [5] Jui-Liang, Ding-Tsair Su, Ying-ShingShiao, Research on MPPT and Single-Stage Grid-Connected for Photovoltaic System, *Wseas Transactions on Systems*, Volume 7, October 2008.
- [6] M. Guisser, A. EL-Jouni, EL. H. Abdelmounim, Robust Sliding Mode MPPT Controller Based on High Gain Observer of a Photovoltaic Water Pumping System, *International Review of Automatic Control*, Vol 7, No 2, 2014.
- [7] M. Guisser, A. EL-Jouni, M. Aboulfatah, E. Abdelmounim, Nonlinear MPPT Controller for Photovoltaic Pumping System Based on Robust Integral Backstepping Approach, *International Review on Modelling and Simulation*, Vol 7, No 3, 2014.
- [8] Hassan Abouobaida, Mohamed Cherkaoui, Robust controller for interleaved DC-DC converters and buck inverter in Grid-Connected Photovoltaic Systems, *Wseas Transactions on Power Systems*, Volume 6, January 2011.
- [9] AbdelhafidAitAlmahjoub , A.Ailane , M.Rachik , A.Essadki, J.Bouyaghroumni, Non-linear Control of a Multi-loop DC-AC Power Converter Using in Photovoltaic System Connected to the Grid, *International Journal of Electrical & Computer Sciences*, Vol 12, No 4, 2012.
- [10] F. L. Albuquerque, A. J. Moraes, G. C. Guimarks, S. M. R. Sanhueza, optimization of a photovoltaic system connected to electric power grid, *IEEE transaction and didtribution conference and exposition*, pp. 645-650. Latin American, 2004.
- [11] Jianxing Liu, Salah Laghrouche, and MaximeWack, Observer-Based Higher Order Sliding Mode Control of Unity Power Factor in Three-Phase AC/DC Converter for Hybrid Electric Vehicle Applications, *International Journal of Control*, 2013.
- [12] M.Makhlouf, F.Messai, H.Benalia, Modeling and control of a single-phase grid connected photovoltaic system, *Journal of Theoretical and Applied Information Technology*, Vol. 37, No.2, March 2012.
- [13] G. Bornard, H. Hammouri, A high gain observer for a class of uniformly observable systems, In: *Proc. 30th IEEE Conference on DecisionandControl*. Vol. 122. Brighton, England. 1991.
- [14] K. Busawon, M. Farza, H. Hammouri, Observer design for a special class of nonlinear systems, *International Journal of Control* 71(3), 405–418, 1998.
- [15] F. L. Liu , M. Farza, M. M’Saad and H. Hammouri, Observer Design for a class of uniformly observable MIMO nonlinear systems with coupled structure, *Proceedings of the 17th World Congress The International Federation of Automatic Control*, Seoul, Korea, July 6-11, 2008.
- [16] M. Hou, K. Busawon and M. Saif, Observer design for a class of MIMO nonlinear systems, *IEEE Trans. on Aut. Control*, 45(7):1350–1355, 2000.
- [17] H. Hammouri and J. De Leon Morales, Observer synthesis for state affine systems, *Proc. 29th IEEE Conf. Decision Control*, pp. 784–785, 1990.
- [18] G. Bornardand N. Couenne, F. Celle, Regularly persistent observer for bilinear systems, In *Proc. 29th International Conference, New Trends in Nonlinear Control Theory*, Volume 122, page 130140, Nantes, France, Springer Verlag, 1998.